Throughput Enhancements on Cellular Downlink Channels using Rateless Codes

Amogh Rajanna and Martin Haenggi
Wireless Institute, University of Notre Dame, USA. {arajanna,mhaenggi}@nd.edu

***Abstract*—Rateless codes have been shown to provide robust error correction over wireless channels. Using a stochastic geometry model, this paper studies the performance of cellular downlink with packet transmission based on rateless codes. For the case of Rayleigh fading, a novel and accurate approximation is proposed for the distribution of the packet transmission time of rateless codes. The performance of rateless codes is compared to that of fixed rate codes by evaluating the user rate and success probability achievable with the two schemes. Based on both the proposed analysis and network simulation, the paper shows that rateless coding provides a throughput gain relative to fixed rate coding, not only for the typical user but for all users in the cellular network.**

I. Introduction

Rateless codes have generated a lot of interest as a promising forward error correction (FEC) technique [1]. Being able to adapt both the code construction and the number of parity symbols to time-varying channel conditions, rateless codes hold the potential for achieving the capacity with relatively short delays compared to fixed rate codes, which have fixed code construction and codeword length [1], [2]. This paper was mainly motivated by the works of [3], [4]. Using tools from stochastic geometry, [3] shows that rateless codes lead to performance improvements in a single hop wireless ad hoc network (WANET). A robust scheme based on rateless codes was proposed to achieve the ergodic rate density (ERD) in a WANET. The Poisson rain model was used to show that rateless codes enable the WANET to achieve a higher rate density and have *near* ERD performance with significantly shorter delays than fixed rate codes. In [4], the meta distribution of SIR is proposed as a powerful tool to study the per-user performance. The meta distribution of the SIR is the success probability of packet transmission conditioned on the point process. It reveals fine-grained information on the per-user performance which, in turn, leads to insights on packet end-to-end delay, QoS levels and congestion across the network. Since rateless codes result in rates that are matched to the instantaneous channel, studying their performance in a framework similar to [4] will lead to new insights in cellular network design.

Using a stochastic geometry model, we characterize the performance of cellular downlink channels when rateless codes are used for FEC and compare it to the case of conventional fixed rate codes. We quantify the distribution of the packet transmission time of rateless codes, defined as the number of channel uses to successfully transmit a K-bit information packet. The analytical result leads to expressions for coverage (success) probability and rate on the cellular downlink and allows a comparison of rateless codes with fixed rate codes. We show that with rateless codes, the success probability and rate on cellular downlink increases substantially relative to fixed rate codes, and we provide expressions for the gain as a function of system parameters. Simulation results indicate that every user in the cellular downlink has a throughput gain under the proposed scheme irrespective of its location within a cell. The closer a user is to the serving BS, the higher the gain.

II. System Model

We consider a cellular network in which BSs are modeled by a homogeneous Poisson point process (PPP) $\Phi = \{X_i\},\ i = 0, 1, 2, \cdots$ of intensity λ. It is assumed that each BS X_i communicates with one user randomly located in its Voronoi cell. The user is located at Y_i. The distance between X_i and its served user Y_i is D_i. Every BS wishes to communicate K bits to its associated user. When the BS X_i is communicating to its user Y_i, all other BSs interfere until they have completed their own transmission. Each BS encodes the K information bits using an ideal variable-length code i.e., rateless code. Each BS uses constant transmit power ρ.

The propagation channel is affected by path loss and small scale fading. We assume a quasi-static flat fading channel, i.e., each packet of K bits is encoded and transmitted within a single coherence time over a Rayleigh block fading channel. (On frequency selective fading, OFDM transmission is present along with rateless coding). For a coherence time T_c and signal bandwidth W_c, each packet transmission of K bits has a delay constraint of $N = T_c W_c$ channel uses. Let T_i denote the packet transmission time of BS X_i to its user Y_i. Starting from channel use 1, each BS X_i has up to N channel uses to transmit a K-bit packet, i.e., $0 < T_i \leq N$. The medium access control (MAC) state of BS X_i at time t is given by $e_i(t) = 1\,(0 < t \leq T_i)$, where $1(\cdot)$ is the indicator function.

The received signal at user Y_i is given by

$$y_i(t) = h_{ii} D_i^{-\alpha/2} x_i + \sum_{k \neq i} h_{ki} |X_k - Y_i|^{-\alpha/2} e_k(t) x_k + z_i,\ 0 < t \leq T_i, \tag{1}$$

where α is the path loss exponent, 1^{st} term represents the desired signal from BS X_i and the 2^{nd} term represents the interference from BSs $\{X_k\}, k \neq i$.

The interference power and SINR at user Y_i at time t are given by

$$I_i(t) = \sum_{k \neq i} \rho |h_{ki}|^2 |X_k - Y_i|^{-\alpha} e_k(t) \tag{2}$$

and

$$\mathrm{SINR}_i(t) = \frac{\rho |h_{ii}|^2 D_i^{-\alpha}}{1 + I_i(t)}, \tag{3}$$

respectively. For brevity, the noise power in (3) is set to 1.

The time averaged interference at user Y_i up to time t is given by

$$\hat{I}_i(t) = \frac{1}{t} \int_0^t I_i(\tau) \ \mathrm{d}\tau. \tag{4}$$

We assume user Y_i employs a nearest-neighbor decoder performing minimum Euclidean distance decoding based on only CSIR [5], then the achievable rate $C_i(t)$ is

$$C_i(t) = \log_2 \left(1 + \frac{\rho |h_{ii}|^2 D_i^{-\alpha}}{1 + \hat{I}_i(t)} \right). \tag{5}$$

Every interfering BS transmits a K bit packet to its user and after receiving the acknowledgment (ACK) signal becomes silent leading to a monotonic interference, i.e., both $I_i(t)$ and $\hat{I}_i(t)$ are decreasing functions of t. Based on (5), the time to decode K information bits and thus the packet transmission time T_i are given by

$$\hat{T}_i = \min \{ t : K < t \cdot C_i(t) \} \tag{6}$$

$$T_i = \min \left(N, \hat{T}_i \right). \tag{7}$$

A characterization of the distribution of the packet time T_i in (7) is essential to quantify the performance advantages of using rateless codes for FEC in a cellular network.

III. Packet Transmission Time

To study the distribution of the packet time, consider the typical user located at the origin. Using a nearest neighbor decoder, the typical user also achieves $C(t)$ in (5). To characterize the CCDF of the packet transmission time T, we first note that the CCDFs of T and $\hat{T}$ are related as

$$\mathbb{P}(T > t) = \begin{cases} \mathbb{P}\left(\hat{T} > t\right) & t < N \\ 0 & t \geq N. \end{cases} \tag{8}$$

Next we consider the two events

$$\mathcal{E}_1(t) : \hat{T} > t$$

$$\mathcal{E}_2(t) : \frac{K}{t} \geq \log_2 \left(1 + \frac{\rho |h|^2 D^{-\alpha}}{1 + \hat{I}(t)} \right). \tag{9}$$

Based on standard information theoretic results, a key observation is that for a given t, the event $\mathcal{E}_1(t)$ is true if and only if $\mathcal{E}_2(t)$ holds true. Thus

$$\mathbb{P}\left(\hat{T} > t\right) = \mathbb{P}\left(\frac{K}{t} \geq \log_2 \left(1 + \frac{\rho |h|^2 D^{-\alpha}}{1 + \hat{I}(t)} \right) \right) \tag{10}$$

$$= \mathbb{P}\left(\frac{\rho |h|^2 D^{-\alpha}}{1 + \hat{I}(t)} \leq 2^{K/t} - 1 \right). \tag{11}$$

Assuming a high enough BS density λ, we ignore the noise term for the remainder of the paper. We let $\theta_t = 2^{K/t} - 1$ and, without loss of generality, set $\rho = 1$. (11) can be written out as

$$\mathbb{P}\left(\hat{T} > t\right) = \mathbb{E}\left[1 - \mathbb{P}\left(\frac{|h|^2 D^{-\alpha}}{\hat{I}(t)} \geq \theta_t \middle| D \right) \right]$$

$$\stackrel{(a)}{=} \mathbb{E}\left[1 - \mathcal{L}_{\hat{I}(t)}\left(\theta_t D^{\alpha} \right) \right], \tag{12}$$

where (a) follows from Rayleigh fading and $\mathcal{L}_Y(s) = \mathbb{E}\left[e^{-sY}\right]$ is the Laplace transform of random variable Y.

An expression for $\hat{I}(t)$, the average interference up to time t at the typical user, can be obtained from (4):

$$\hat{I}(t) = \sum_{k \neq 0} |h_k|^2 |X_k|^{-\alpha} \eta_k(t) \tag{13}$$

$$\eta_k(t) = \frac{1}{t} \int_0^t e_k(\tau) \ \mathrm{d}\tau = \min(1, T_k/t). \tag{14}$$

The marks $\eta_k(t)$ are correlated for different k, which makes it impossible to find the exact CCDF in (12).

In the following, two approaches to study the CCDF are discussed.

A. Lower Bound

From (11), the CCDF can be lower bounded by considering a lower bound to the interference $\hat{I}(t)$. Hence we consider the nearest-interferer lower bound to $\hat{I}(t)$.

$$\mathbb{P}\left(\hat{T} > t\right) = \mathbb{P}\left(\frac{|h|^2 D^{-\alpha}}{\hat{I}(t)} \leq \theta_t \right)$$

$$\stackrel{(a)}{\geq} \mathbb{P}\left(\frac{|h|^2 D^{-\alpha}}{I(t)} \leq \theta_t \right)$$

$$\geq \mathbb{P}\left(\frac{|h|^2 D^{-\alpha}}{|h_1|^2 |X_1|^{-\alpha} \ 1(t \leq T_1)} \leq \theta_t \right) \tag{15}$$

$$\stackrel{(b)}{=} \underbrace{\mathbb{P}\left(\frac{|h|^2 D^{-\alpha}}{|h_1|^2 |X_1|^{-\alpha}} \leq \theta_t \right)}_{P_1} \underbrace{\mathbb{P}(t \leq T_1)}_{P_2}, \tag{16}$$

where in (a) $I(t)$ is the instantaneous interference at time t, which is monotonically decreasing with t, and hence, $\hat{I}(t) \geq I(t)$. Splitting (15) by conditioning on the event $t \leq T_1$ and its complement $t > T_1$ leads to (b).

Let T_{ni} be the packet transmission time based on interference from *only* the nearest interferer with the assumption that it is always ON.

In the following, the distribution of T_{ni} is given.

Proposition 1. *The CCDF of T_{ni} is given by*

$$\mathbb{P}(T_{\mathrm{ni}} > t) = 1 - {}_2F_1([1, \delta]; 1 + \delta; -\theta_t), \tag{17}$$

where ${}_2F_1([a,b];c;z)$ is the Gauss hypergeometric function, $\delta = 2/\alpha$ and $\theta_t = 2^{K/t} - 1$.

Proof: Similar to (10), the CCDF of T_{ni} is given by

$$\mathbb{P}(T_{\mathrm{ni}} > t) = \mathbb{P}\left(\frac{K}{t} \geq \log_2 \left(1 + \frac{|h|^2 D^{-\alpha}}{|h_1|^2 |X_1|^{-\alpha}} \right) \right). \tag{18}$$

To compute (18), let $V = D/|X_1|$. The distribution of V is known [6, Lemma 3].

$$\begin{aligned}\mathbb{P}\left(T_{\text{ni}} > t\right) &= \mathbb{P}\left(\frac{|h|^2}{|h_1|^2} V^{-\alpha} \leq \theta_t\right) \\ &= 1 - \mathbb{E}\left[\mathbb{E}\left[\exp\left(-\theta_t |h_1|^2 V^{\alpha}\right) \Big| V\right]\right] \\ &= 1 - \mathbb{E}\left[\frac{1}{1+\theta_t V^{\alpha}}\right] \\ &= 1 - \int_0^1 \frac{1}{1+\theta_t v^{\alpha}} \, \mathrm{d}v^2 \\ &= 1 - \int_0^1 \frac{\delta y^{\delta-1}}{1+\theta_t y} \, \mathrm{d}y \\ &= 1 - {}_2F_1\left([1,\delta]; 1+\delta; -\theta_t\right).\end{aligned} \tag{19}$$

■

Note that the CCDF of T_{ni} in Proposition 1 is the same as the term P_1 in (16). $P_2 = \mathbb{P}\left(t \leq T_1\right)$ is the probability that the nearest-interferer X_1 transmits up to time t and unfortunately it does not seem possible to find an expression. However, in the next subsection, we illustrate the applicability of P_1 in (17) to study the distribution of the typical user's packet transmission time.

B. Independent Thinning Approximation

To characterize the dependence of the typical user's transmission time on the time varying interference of the cellular network, we make a simplifying approximation. The assumption is that the interfering BSs transmit for a random duration $\bar{T}_k$ from time $t = 0$ and then become inactive, irrespective of their packet success or failure. Statistically the $\bar{T}_k$ are assumed iid with CDF $F(\bar{t})$ and hence this approximation is termed independent thinning model. Under this model, the instantaneous interference at typical user can be written as

$$\tilde{I}\left(t\right) = \sum_{k \neq 0} |h_k|^2 |X_k|^{-\alpha} 1\left(t \leq \bar{T}_k\right). \tag{20}$$

The time averaged interference at the typical user is given by

$$\begin{aligned}\bar{I}\left(t\right) &= \sum_{k \neq 0} |h_k|^2 |X_k|^{-\alpha} \bar{\eta}_k(t) \\ \bar{\eta}_k(t) &= \min\left(1, \bar{T}_k/t\right).\end{aligned} \tag{21}$$

From now onwards, we just use $\bar{\eta}$ instead of $\bar{\eta}(t)$ for brevity.

Under the independent thinning model, the typical user packet transmission time T is

$$\begin{aligned}\hat{T} &= \min\left\{t : K < t \cdot \log_2\left(1 + \frac{|h|^2 D^{-\alpha}}{\bar{I}(t)}\right)\right\} \\ T &= \min\left(N, \hat{T}\right).\end{aligned} \tag{22}$$

The CCDF of the typical user's packet transmission time T in (22) is bounded in the following theorem.

Theorem 1. *An upper bound on the CCDF of typical user packet transmission time under the independent thinning model, T in (22), is given by*

$$\mathbb{P}\left(T > t\right) \leq \begin{cases} P_{\text{ub}}(t) & t < N \\ 0 & t \geq N, \end{cases} \tag{23}$$

where

$$P_{\text{ub}}(t) = 1 - \frac{1}{{}_2F_1\left([1,-\delta]; 1-\delta; -\theta_t \min\left(1, \mu/t\right)\right)}, \tag{24}$$

and

$$\mu = \int_0^N \left(1 - {}_2F_1\left([1,\delta]; 1+\delta; 1-2^{K/t}\right)\right) \mathrm{d}t. \tag{25}$$

Proof: See Appendix A. ■

The CCDF of packet transmission time from the independence thinning approximation in Theorem 1 serves as a simplified model of the exact cellular network in (7). The predicted performance of cellular network from the results of Theorem 1 will be compared to the actual cellular network performance through simulation in Section V.

IV. Performance Comparison

In this section, we outline a methodology to quantify the benefits of using rateless codes by studying the performance of a cellular network under two scenarios. In one scenario, the cellular network employs rateless codes for FEC while in the second scenario, conventional fixed rate codes are used for FEC.

When the cellular network uses fixed rate codes for FEC, each BS encodes a K bit information packet using a fixed rate code, e.g., an LDPC code or turbo code and transmits the entire codeword of N parity symbols. The user receives the N parity symbols over the downlink channel and tries to decode the information packet using the BCJR or Viterbi algorithm. Depending on the instantaneous channel conditions, the single decoding attempt may be successful or not.

When the cellular network uses rateless codes for FEC, each BS encodes a K bit packet using a variable length code, e.g., a Raptor code or a LT-concatenated code [1]. The parity symbols are incrementally generated and transmitted until K bits are decoded at the user or the maximum number of parity symbols N is reached. The user performs multiple decoding attempts to decode the information packet using the Belief Propogation or Sum-Product algorithm. An outage occurs if K bits are not decoded within N parity symbols.

The metrics used to compare the performance of the two FEC approaches are the typical user rate and success probability, which are defined below for both fixed rate coding and rateless coding schemes.

A. Fixed Rate Coding

The SIR threshold for fixed rate coding is given by $\theta = 2^{K/N} - 1$. The SIR of the typical user is obtained from (2) and (3) with $e_k(t) = 1$ for all k (and ignoring the noise term).

The success probability and rate of the typical user are defined and given as

$$p_{\rm s}(N) \triangleq \mathbb{P}\left(\mathrm{SIR} > 2^{K/N}-1\right) = \frac{1}{{}_2F_1\left([1,-\delta]\,;1-\delta;1-2^{K/N}\right)}. \quad (26)$$

$$R_N \triangleq p_{\rm s}(N)\log_2(1+\theta) = \frac{K/N}{{}_2F_1\left([1,-\delta]\,;1-\delta;1-2^{K/N}\right)}. \quad (27)$$

The two terms in R_N exhibit a tradeoff as a function of N, namely the success probability $p_{\rm s}(N)$ is increasing and the rate $\log_2(1+\theta)$ is decreasing with N. Let $N_{\rm f}$ be the optimal value of N to maximize R_N in (27).

B. Rateless Coding

The SIR threshold for rateless coding at time t is given by $\theta_t = 2^{K/t}-1$. The success probability and rate of the typical user are defined as

$$p_{\rm s}(N) \triangleq 1-\mathbb{P}\left(\hat{T}>N\right) \quad (28)$$

$$R_N \triangleq \frac{Kp_{\rm s}(N)}{\mathbb{E}\left[T\right]}. \quad (29)$$

Note that as per (7), T is a truncated version of $\hat{T}$ at N. Let $N_{\rm r}$ be the optimal value of N to maximize R_N in (29). The complement of the success probability in (26) and (28) is the information outage probability, interpreted as the limiting value of the probability of decoding error of specific channel codes for large codeword length [7].

In the following, we quantify the performance gains of using rateless codes.

Proposition 2. *The success probability gain of rateless codes relative to fixed rate codes under the independent thinning model is bounded as*

$$G_{\rm s} \geq \frac{{}_2F_1\left([1,-\delta]\,;1-\delta;1-2^{K/N}\right)}{{}_2F_1\left([1,-\delta]\,;1-\delta;\left(1-2^{K/N}\right)\mu/N\right)}. \quad (30)$$

Proof: The gain is obtained by taking the ratio of success probabilities for both rateless coding and fixed rate coding. Under the independent thinning model, the success probability for rateless coding can be obtained by combining (40)-(42) at $t=N$, which yields

$$\tilde{p}_{\rm s}(N) \geq \frac{1}{{}_2F_1\left([1,-\delta]\,;1-\delta;-\theta\min\left(1,\mu/N\right)\right)}. \quad (31)$$

Taking the ratio of above $\tilde{p}_{\rm s}(N)$ to that in (26) yields the $G_{\rm s}$ in (30). Note that $\mu < N$ always and hence, $G_{\rm s} > 1$. ∎

The SIR threshold θ is valuable to assess the performance gain in a cellular network [8]. Hence one interpretation of (30) is given below.

Corollary 1. *Rateless coding in cellular downlink leads to a SIR gain of $\frac{N}{\mu}$ relative to fixed rate coding.*

Remark: The SIR threshold θ is reduced by a factor $\frac{N}{\mu}$ and hence, the above result under independent thinning proves that rateless coding leads to improved coverage on cellular downlink. Note that from (25), μ/N depends on path loss exponent α and fixed rate K/N.

To compute the rate in (29) analytically, the expected packet time is bounded as

$$\mathbb{E}\left[T\right] \leq \int_0^N P_{\rm ub}(t)\ \mathrm{d}t, \quad (32)$$

where $P_{\rm ub}(t)$ is obtained from Theorem 1.

Proposition 3. *The rate gain in cellular downlink when rateless codes perform FEC relative to fixed rate codes under the independent thinning model is*

$$G_{\rm r} = G_{\rm s}\ \frac{N}{\mathbb{E}\left[T\right]}. \quad (33)$$

Comparing the rates in (27) and (29) gives the above result. Note that $\frac{N}{\mathbb{E}[T]} > 1$ can be viewed as a gain in packet time. The packet time and success probability gains act in tandem to produce a rate gain $G_{\rm r} > 1$. However, it does not seem possible to simplify $G_{\rm r}$ further.

The claims of Propositions 2 and 3 are numerically validated in Section V.

V. Numerical Results

In this section, we present numerical results that illustrate the performance benefits of using rateless codes for FEC in a cellular network. Inspired by [4], the numerical results are presented under two frameworks in the subsections below, with one offering insights into the typical user performance while the other provides a higher level of detail.

A. Spatial Averaged Performance

In this framework, computing either success probability or rate based on (26) to (29) involves spatial averaging of the performance metric over the PPP. This computation can be accomplished both by simulation and the analytic expressions in Sections IV-A and IV-B. For the simulation, the cellular network was realized on a square of side 60 with wrap around edges. The BS PPP intensity is $\lambda = 1$. The information packet size is $K = 75$ bits. The cellular network performance was evaluated for varying path loss exponent α and delay constraint N. The network is simulated as per the exact model described in (2)-(7) while the independent thinning model of Section III-B is used for analysis.

In Fig. 1, the success probability is plotted as a function of the delay constraint for both fixed rate coding and rateless coding based on (26) and (31). It is observed that for $\alpha \in \{3,4\}$, rateless coding leads to a higher success probability relative to fixed rate coding. In a cellular network with rateless coding, BSs with good channel conditions transmit the K bits to their users with small to moderate packet time and turn OFF. This process reduces the interference for the remaining BSs, allowing them to communicate to their users with improved SIR conditions. Hence for a given N, a cellular network

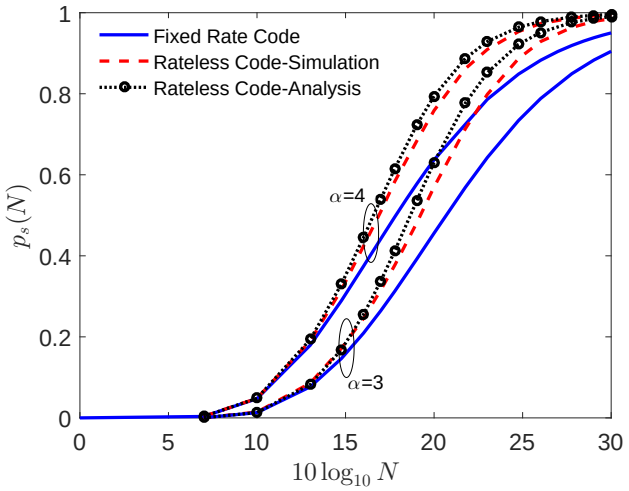

Fig. 1. The success probability as a function of the delay constraint N in a cellular network with $\lambda = 1$ at $\alpha = 3$ and $\alpha = 4$ for both fixed rate coding and rateless coding based on (26) and (31) respectively.

with rateless coding has a higher number of successful packet transmissions relative to fixed rate coding.

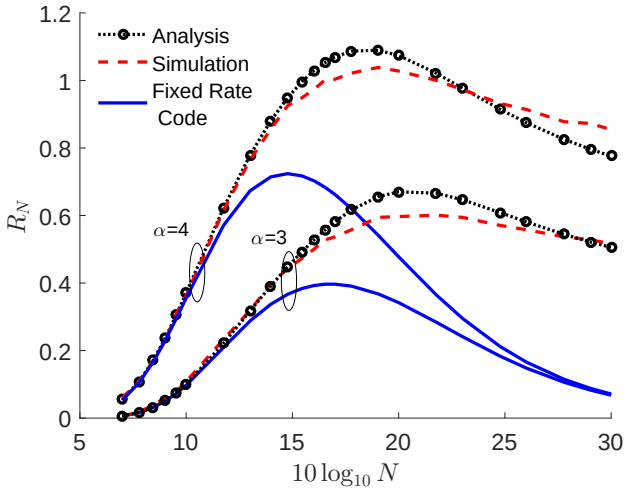

Fig. 2. The typical user rate R_N in a cellular network with $\lambda = 1$ as a function of N. For fixed rate coding, the rate is based on (27) while for rateless coding, the approximation is obtained by combining (29), (31) and (32).

Fig. 2 shows the rate R_N for both fixed rate coding and rateless coding as a function of N. For both schemes, there is an optimal N which maximizes the rate, balancing the tradeoff between increasing $p_s(N)$ and $\mathbb{E}[T]$ (or N for fixed rate coding). For rateless coding, the success probability increases faster, and the expected packet time grows slowly with N relative to fixed rate coding. Hence it is observed that N_r is higher than N_f, and the maximal rate for rateless coding is higher than that of fixed rate coding. The N_r from simulation and analytical results of Theorem 1 match very well, validating the proposed independent thinning model.

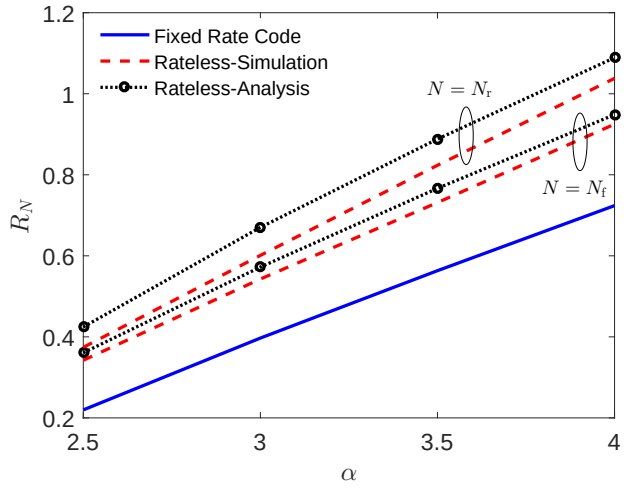

Fig. 3. The typical user rate in a cellular network with $\lambda = 1$ for both fixed rate coding and rateless coding against the path loss exponent α. For each α, the typical user rate for rateless coding at both values N_f and N_r are plotted.

Fig. 3 plots the typical user rate as a function of the path loss exponent α. For fixed rate coding, at each α, the typical user rate is computed at the maximizing N_f. For rateless coding, the rate at both values N_f and N_r are plotted. Fig. 3 clearly illustrates the performance advantage of using rateless codes. At each α, it is observed that the throughput gain is approximately constant when operating at either N_f or N_r.

B. Per-user Performance

The numerical results in the previous subsection provide the performance of the typical user, which is the spatial average of all users performance. While the spatial averages allow to compare the performance of rateless coding to fixed rate coding, they do not reveal the behavior of individual BS-UE pairs in a given network realization [4]. How does a user near to (or far from) the BS benefit from rateless coding? In this subsection, we attempt to answer the question by focusing on the per-user performance in a given network realization. The numerical results presented are based purely on simulation.

Fig. 4 shows a snapshot of a cellular network with BSs and users represented by $\times$ and $\circ$ respectively. For this network realization, the rates achieved by each BS-UE pair for both FEC schemes is computed. Since the network is fixed, the rates are averaged only over fading. For each pair, the rate for rateless coding is shown first while that for fixed rate coding is below it. It is observed that the users very close to their serving BS achieve the most benefit.

The insights from Fig. 4 are verified in Fig. 5, which shows the ratio of rates of the two FEC schemes for every BS-UE pair in the cellular network as a function of the BS-UE distance. This plot illustrates that *every user in the cellular network with PPP realization has a throughput gain* > 1 *by using rateless codes*. Since a PPP is inclusive of other point processes, the insight from Fig. 5 is very supportive of using rateless codes for FEC. On average, it may appear that the

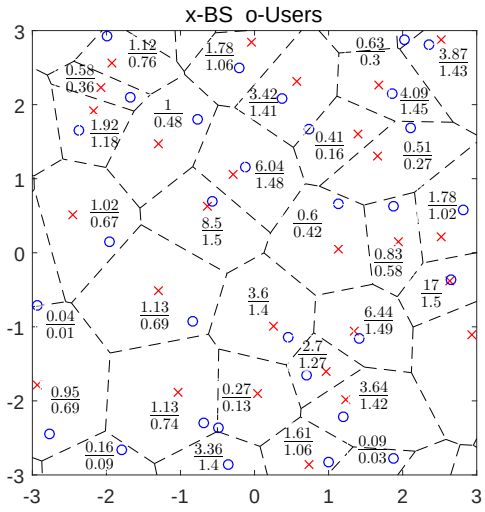

Fig. 4. Rates of BS-UE pairs in a realization of a cellular network with $\lambda = 1$ at $\alpha = 4$ and $N = 50$. For each pair, a ratio of rates is shown. The rate for rateless coding is shown at the top and that for fixed rate coding is shown below it.

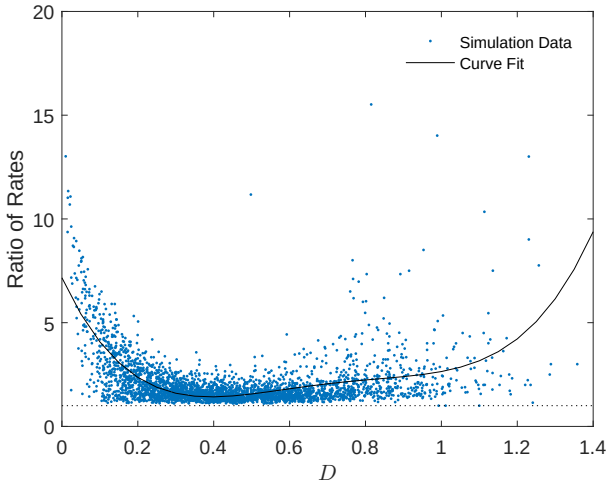

Fig. 5. The ratio of rate with rateless coding to the rate with fixed rate coding for every BS-UE pair as a function of the BS-UE distance D in a cellular network realization with $\lambda = 1$ at $\alpha = 4$ and $N = 50$.

closer a user is to its serving BS, the larger its gain. But more details can be obtained from Fig. 5. For a given value of D, it is observed that different BS-UE pairs can possibly achieve different throughput gains. For example, the BS-UE pairs with a distance of 0.1 may achieve a gain anywhere from 1 to around 7. Similarly for a distance of 0.6, the gains can be from 1 to 4. For a given value of D, the plotted rates are averaged over the fading process and hence the gains depend on the interferer locations. For a fixed D, smaller cells have nearby interferers leading to a lower gain whereas bigger cells have interferers further away and hence achieve a higher gain.

Fig. 6 plots the per-user rates for rateless coding and fixed rate coding against the BS-UE distance D at $\alpha = 3$ and

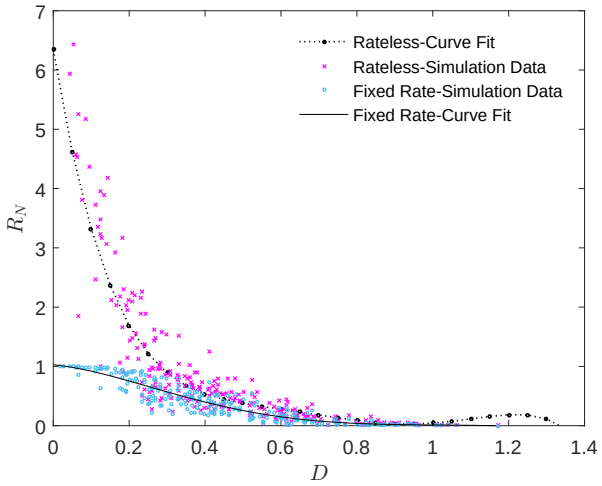

Fig. 6. The per-user rates for rateless coding and fixed rate coding in a cellular network realization as a function of D at $\alpha = 3$ and $N = 75$.

$N = 75$. Again the network realization is fixed. Since rateless codes adapt the amount of redundancy to instantaneous channel conditions, i.e., BS-UE distance and interferer locations in Fig. 6, the users close to the serving BS get much higher rates under rateless coding relative to fixed rate coding with fixed redundancy. For a given network realization, these higher per-user rates under rateless coding lead to positive effects on network congestion, packet end-to-end delay, and QoS levels. In terms of implementation complexity, the number of XOR operations for encoding and decoding grow only linearly with the packet size for a Raptor code and quadratically for a Reed-Solomon code.

VI. Conclusion

The paper proposes rateless codes as a viable FEC technique in a cellular downlink setting and investigates its advantage over fixed rate codes. An independent thinning model was proposed to study the effects of time varying interference on the packet transmission time. The potential of rateless codes to improve coverage probability, provide a throughput gain for every user in the network, and achieve per-user rates which lead to efficient network operation relative to fixed rate codes was demonstrated through numerical results representing both spatial averaged and per-user performance measures for practically significant network scenarios.

Appendix A
Proof of Theorem 1

From (8), the CCDF of T is the same as the CCDF of $\hat{T}$ when $t < N$ and is 0 elsewhere.

The CCDF of $\hat{T}$ has the same form as in (12) with the interference term being replaced by $\bar{I}(t)$ in (21), for which the Laplace transform $\mathcal{L}(\cdot)$ is given by [9]

$$\mathcal{L}_{\bar{I}(t)|D}(s) = \exp\left(-\pi\lambda\mathbb{E}_{h,\bar{\eta}}\left[\int_D^\infty \left(1 - e^{-s|h|^2\bar{\eta}v^{-\alpha}}\right) \mathrm{d}v^2\right]\right).$$

Letting $s = \theta_t D^\alpha$,

$$\begin{aligned}
&\mathcal{L}_{\bar{I}(t)|D}\left(\theta_t D^\alpha\right) \\
&= \exp\left(-\pi\lambda\mathbb{E}_{h,\bar{\eta}}\left[\int_D^\infty \left(1 - e^{-\theta_t D^\alpha |h|^2 \bar{\eta} v^{-\alpha}}\right) \mathrm{d}v^2\right]\right) \\
&= \exp\left(-\pi\lambda\mathbb{E}_{\bar{\eta}}\left[\int_D^\infty \left(1 - \frac{1}{1+\theta_t\left(D/v\right)^\alpha \bar{\eta}}\right) \mathrm{d}v^2\right]\right) \\
&\overset{(a)}{=} \exp\left(-\pi\lambda D^2 \delta\theta_t^\delta \mathbb{E}\left[\int_0^{\theta_t} \left(1 - \frac{1}{1+\bar{\eta}y}\right) \frac{\mathrm{d}y}{y^{1+\delta}}\right]\right),
\end{aligned} \tag{34}$$

where (a) follows from the substitution $y = \theta_t \left(D/v\right)^\alpha$.

For notational simplicity in (34), we define

$$H(t) \triangleq \delta\theta_t^\delta \mathbb{E}\left[\int_0^{\theta_t} \left(1 - \frac{1}{1+\bar{\eta}y}\right) \frac{1}{y^{1+\delta}}\,\mathrm{d}y\right]. \tag{35}$$

Using the fact that $D \sim \text{Rayleigh}\left(1/\sqrt{2\pi\lambda}\right)$, from (12) the CCDF of $\hat{T}$ is given as

$$\begin{aligned}
\mathbb{P}\left(\hat{T} > t\right) &= \mathbb{E}\left[1 - \exp\left(-\pi\lambda H(t) D^2\right)\right] \\
&= 1 - \frac{1}{H(t)+1}.
\end{aligned} \tag{36}$$

The CCDF of $\hat{T}$ depends on the distribution of interferer packet time $\bar{T}$ through the term $H(t)$. In the following, a simple expression for $H(t)$ is derived.

$$\begin{aligned}
H(t) &= \delta\theta_t^\delta \mathbb{E}\left[\int_0^{\theta_t} \frac{\bar{\eta}}{\left[1+y\bar{\eta}\right] y^\delta}\,\mathrm{d}y\right] \\
&= \frac{\theta_t\delta}{1-\delta}\,\mathbb{E}\left[\bar{\eta}\ {}_2F_1\left(\left[1, 1-\delta\right]; 2-\delta; -\theta_t\bar{\eta}\right)\right] \qquad (37) \\
&= \frac{\theta_t\delta}{1-\delta}\left[\int_0^t \frac{\bar{t}}{t}\ {}_2F_1\left(\left[1, 1-\delta\right]; 2-\delta; -\frac{\bar{t}}{t}\theta_t\right) \mathrm{d}F(\bar{t})\right. \\
&\quad \left. + \left(1 - F(t)\right)\ {}_2F_1\left(\left[1, 1-\delta\right]; 2-\delta; -\theta_t\right)\right], \qquad (38)
\end{aligned}$$

where $F(\bar{t}) = \mathbb{P}\left(\bar{T} \le \bar{t}\right)$, which is assumed to be given.

Combining (36) and (38) leads to an expression for the CCDF of $\hat{T}$. Although exact, the expression for $H(t)$ in (38) is computationally intensive since it involves an integral over the hypergeometric function for every value of t.

Hence a simpler upper bound is derived for $H(t)$ by writing it as an expectation over the following function of $\bar{T}$,

$$\begin{aligned}
g\left(\bar{T}\right) &= \frac{1}{1 + y\min\left(1, \bar{T}/t\right)} \\
H(t) &= \delta\theta_t^\delta \int_0^{\theta_t} \mathbb{E}\left[1 - g\left(\bar{T}\right)\right] \frac{1}{y^{1+\delta}}\,\mathrm{d}y.
\end{aligned} \tag{39}$$

The function $g\left(\bar{T}\right)$ is convex in $\bar{T}$. Letting $\mu = \mathbb{E}\left[\bar{T}\right]$, using Jensen's inequality for convex functions results in the following upper bound for $H(t)$ in (39)

$$\begin{aligned}
H(t) &\le \delta\theta_t^\delta \int_0^{\theta_t} \left(1 - g\left(\mu\right)\right) \frac{1}{y^{1+\delta}}\,\mathrm{d}y \\
&= \delta\theta_t^\delta \int_0^{\theta_t} \frac{\min\left(1, \mu/t\right)}{\left[1 + y\min\left(1, \mu/t\right)\right] y^\delta}\,\mathrm{d}y \\
&= \frac{\delta}{1-\delta}\theta_t \min\left(1, \mu/t\right)\ {}_2F_1\Big(\left[1, 1-\delta\right]; \\
&\quad 2-\delta; -\theta_t\min\left(1, \mu/t\right)\Big) \\
&\triangleq H_{\text{ub}}(t).
\end{aligned} \tag{40}$$

Thus combining (36) and (40), an upper bound for CCDF is given by

$$\mathbb{P}\left(\hat{T} > t\right) \le 1 - \frac{1}{H_{\text{ub}}(t)+1}. \tag{41}$$

For $H_{\text{ub}}(t)$ in (40), applying the following hypergeometric identity simplifies the upper bound in (41) and yields (24).

$$\begin{aligned}
&\frac{\delta}{1-\delta}\beta\ {}_2F_1\left(\left[1, 1-\delta\right]; 2-\delta; -\beta\right) + 1 \\
&\qquad \equiv {}_2F_1\left(\left[1, -\delta\right]; 1-\delta; -\beta\right).
\end{aligned} \tag{42}$$

To complete the proof, we need to provide an expression for the mean interferer packet transmission time μ. We specify the interferer packet time distribution to follow the distribution of packet time based on the always ON nearest interferer case given in Proposition 1. Thus,

$$\begin{aligned}
\mu &= \int_0^N \left(1 - {}_2F_1\left(\left[1, \delta\right]; 1+\delta; 1-2^{K/t}\right)\right) \mathrm{d}t \qquad (43) \\
&\overset{(a)}{=} K\log 2 \int_0^\infty \frac{1 - {}_2F_1\left(\left[1, \delta\right]; 1+\delta; 1-v\right)}{v\log^2 v}\,\mathrm{d}v, \quad N \to \infty,
\end{aligned}$$

where (a) follows from $v = 2^{K/t}$.

REFERENCES

[1] N. Bonello, Y. Yang, S. Sonia, and L. Hanzo, "Myths and Realities of Rateless Coding," *IEEE Communications Magazine*, no. 8, pp. 143–151, August 2011.

[2] E. Soljanin, N. Varnica, and P. Whiting, "Punctured vs. Rateless Codes for Hybrid ARQ," in *Proc. IEEE Info. Theory Workshop*, 2006, pp. 155–159.

[3] A. Rajanna, I. Bergel, and M. Kaveh, "Performance Analysis of Rateless Codes in an ALOHA Wireless Adhoc Network," *IEEE Transactions on Wireless Communication*, vol. 14, no. 11, pp. 6216–6229, Nov 2015.

[4] M. Haenggi, "The Meta Distribution of the SIR in Poisson Bipolar and Cellular Networks," *IEEE Transactions on Wireless Communication*, vol. 15, no. 4, pp. 2577–2589, Apr 2016.

[5] A. Lapidoth, "Nearest neighbor decoding for additive non-Gaussian noise channels," *IEEE Transactions on Information Theory*, vol. 42, no. 5, pp. 1520 – 1529, Sept 1996.

[6] X. Zhang and M. Haenggi, "A Stochastic Geometry Analysis of Inter-cell Interference Coordination and Intra-cell Diversity," *IEEE Transactions on Wireless Communication*, vol. 13, no. 12, pp. 6655–6669, Dec 2014.

[7] G. Caire and D. Tuninetti, "The Throughput of Hybrid- ARQ protocols for the Gaussian Collision Channel," *IEEE Transactions on Information Theory*, vol. 47, no. 5, pp. 1971–1988, Jul 2001.

[8] R. K. Ganti and M. Haenggi, "Asymptotics and Approximation of the SIR Distribution in General Cellular Networks," *IEEE Transactions on Wireless Communication*, vol. 15, no. 3, pp. 2130–2143, Mar 2016.

[9] M. Haenggi, *Stochastic Geometry for Wireless Networks*, 1st ed. Cambridge University Press, 2013.